5-2004

Infrared spectrum and stability of a π-type hydrogen-bonded complex between the OH and C2H2 reactants

James B. Davey

Margaret E. Greenslade
University of New Hampshire, Margaret.E.Greenslade@unh.edu

Mark D. Marshall

Marsha I. Lester

Martyn D. Wheeler

Recommended Citation
J. B. Davey, M. E. Greenslade, M. D. Marshall, M. I. Lester, M. D. Wheeler, "Infrared spectrum and stability of a π-type hydrogen-bonded complex between the OH and C2H2 reactants," J. Chem. Phys. 121, 3009 (2004).

Infrared spectrum and stability of a π-type hydrogen-bonded complex between the OH and C2H2 reactants

James B. Davey, Margaret E. Greenslade, Mark D. Marshall, Marsha I. Lester, and Martyn D. Wheeler

Citation: J. Chem. Phys. **121**, 3009 (2004); doi: 10.1063/1.1768933
View online: http://dx.doi.org/10.1063/1.1768933
View Table of Contents: http://jcp.aip.org/resource/1/JCPSA6/v121/i7
Published by the American Institute of Physics.

Infrared spectrum and stability of a π-type hydrogen-bonded complex between the OH and C_2H_2 reactants

James B. Davey,[a] Margaret E. Greenslade, Mark D. Marshall,[b] and Marsha I. Lester[c]
Department of Chemistry, University of Pennsylvania, Philadelphia, Pennsylvania 19104-6323

Martyn D. Wheeler
Department of Chemistry, University of Leicester, Leicester, United Kingdom LE1 7RH

(Received 18 March 2004; accepted 14 May 2004)

A hydrogen-bonded complex between the hydroxyl radical and acetylene has been stabilized in the reactant channel well leading to the addition reaction and characterized by infrared action spectroscopy in the OH overtone region. Analysis of the rotational band structure associated with the *a*-type transition observed at 6885.53(1) cm^{-1} (origin) reveals a T-shaped structure with a 3.327(5) Å separation between the centers of mass of the monomer constituents. The OH ($v=1$) product states populated following vibrational predissociation show that dissociation proceeds by two mechanisms: intramolecular vibrational to rotational energy transfer and intermolecular vibrational energy transfer. The highest observed OH product state establishes an upper limit of 956 cm^{-1} for the stability of the π-type hydrogen-bonded complex. The experimental results are in good accord with the intermolecular distance and well depth at the T-shaped minimum energy configuration obtained from complementary *ab initio* calculations, which were carried out at the restricted coupled cluster singles, doubles, noniterative triples level of theory with extrapolation to the complete basis set limit. © *2004 American Institute of Physics*. [DOI: 10.1063/1.1768933]

I. INTRODUCTION

The reaction of hydroxyl radicals (OH) with acetylene (C_2H_2) is of importance in the degradation of acetylene to CO_2, both in the atmosphere and in diffusion-controlled flames.[1,2] Kinetic studies have shown that the $OH+C_2H_2$ reaction proceeds by electrophilic addition at low temperatures ($T \leqslant 450$ K) to produce the HCCHOH radical intermediate and by hydrogen abstraction at high temperatures ($T \geqslant 1000$ K) to yield C_2H+H_2O. Near room temperature, the dominant mechanism is electrophilic addition of the OH radical to the π bond of acetylene. The addition reaction forms an initially energy-rich HCCHOH* adduct, which can dissociate back to reactants or be collisionally stabilized with bath gas M to the HCCHOH radical intermediate, the latter step giving rise to a pressure dependence.[3]

$$C_2H_2+OH \leftrightarrow HCCHOH^*$$

$$HCCHOH^*+M \rightarrow HCCHOH+M$$

The recommended value for the associated rate constant (in the high pressure limit) is $k^{EXP}=9.0\times10^{-13}$ cm^3 $molecule^{-1}$ s^{-1}.[3] The temperature dependence of the rate constant yields a very small activation energy of only 1.3 kcal mol^{-1} in the high pressure limit.[4]

The stationary points along the addition and abstraction reaction pathways, shown in Fig. 1, have been identified through *ab initio* calculations. Early calculations by Sosa and Schlegel used unrestricted Hartree-Fock and Møller-Plesset perturbation theory to characterize the reactant complexes and transition states for the OH addition reactions to acetylene and ethylene.[5] A reactant complex has been offered as an explanation of the small negative activation energy in the addition of OH to ethylene,[6–9] and may also play a role in the initial addition of OH to acetylene, which has a small positive activation energy. The reactant complexes are predicted to have a T-shaped structure with the H atom of OH pointing toward the π bond of acetylene or ethylene. The OH-acetylene complex was computed to have a well depth between 2.4 and 3.2 kcal mol^{-1} at a center-of-mass separation of ~3.5 Å with about 1.0 kcal mol^{-1} of zero-point energy.[5] Significantly higher level *ab initio* calculations of the OH-acetylene reactant complex are carried out as part of the present study, which complement the first experimental investigation of the OH-acetylene complex that is the primary focus of this paper.

The predicted structure of the transition state (TS1) for the addition reaction differs from the reactant complex primarily in the orientation of the OH radical with respect to the acetylene molecule. In the reactant complex, OH lies perpendicular to the π bond of acetylene, while at the transition state the O atom of the OH radical is rotated toward the carbon atom to facilitate forming the new C–O bond.[5,10] The barrier height was not well determined in early *ab initio* calculations,[5] but more recent high-level calculations place the classical barrier height with zero-point corrections at 2.7 kcal mol^{-1} above the reactant asymptote.[10] The transition state (TS2) for the hydrogen abstraction reaction is predicted to lie significantly higher than TS1 (Ref. 10) and, as a result,

[a]Current address: Department of Chemistry, University of Leeds, Leeds, UK LS2 9JT.
[b]On sabbatical leave from Department of Chemistry, Amherst College, P.O. Box 5000, Amherst, MA 01002-5000.
[c]Author to whom correspondence should be addressed; FAX: (215) 573-2112. Electronic mail: milester@sas.upenn.edu

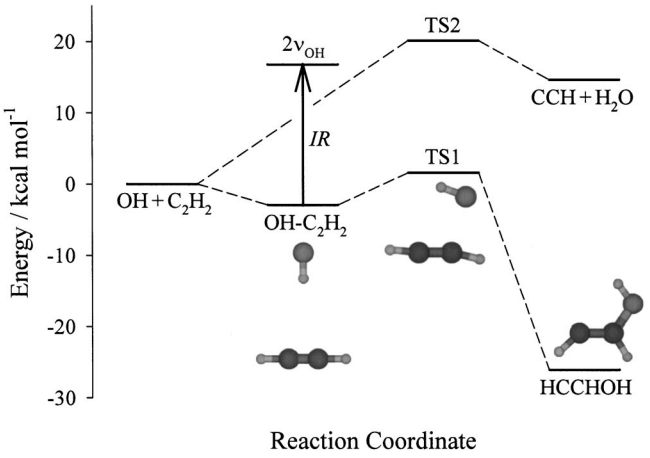

FIG. 1. Schematic pathways for the OH and C_2H_2 addition and abstraction reactions. The properties of the transition states are obtained from *ab initio* theory,[5,10] while those of the reactant complex are determined from this and previous studies.[5] The more stable of two isomers of the radical intermediate HCCHOH is depicted as the addition product.[5,10] Infrared excitation (IR) of the OH-acetylene complex on the OH overtone transition provides enough energy to surmount the barrier to the addition reaction (TS1), but not the abstraction reaction (TS2), and break the weak intermolecular bond. The latter produces OH ($v=1$) fragments, which are detected with the UV probe laser.

this channel is not expected to play a role in the present study.

This paper focuses on the identification and characterization of a hydrogen-bonded complex between the reactants that is associated with the initial addition of the OH radical to acetylene. The structure and stability of this complex are investigated through infrared action spectra of the OH-acetylene complex in the OH overtone region. This excitation provides sufficient energy to surmount the barrier for the addition reaction (TS1), but not the abstraction reaction (TS2), and can also induce vibrational predissociation of the complex. The latter produces OH fragments that can be detected with high selectivity and sensitivity. Additional experimental studies of the OH-acetylene complex have been carried out in the asymmetric stretching region of acetylene; these results will be presented elsewhere because of the complexity of the spectral data.[11]

A related paper by Marshall and Lester develops a theoretical model to interpret the experimental OH-acetylene spectra, which accounts for the coupling of the OH orbital and spin angular momenta with overall rotational motion in a rigidly T-shaped complex.[12] A comparison of model calculations with experimental spectra, particularly in the asymmetric acetylenic stretch region,[11] shows that the OH radical's orbital angular momentum is partially quenched in the OH-acetylene complex. The significant interaction between the OH radical and acetylene in nonlinear configurations, specifically the change in the intermolecular potential with orientation of the half-filled $p\pi$ orbital of OH, gives rise to this quenching. This phenomenon has not been observed previously in more weakly bound complexes of OH $X\,^2\Pi$ with inert or reactive partners, but is expected to become a general feature of more strongly interacting radical-molecule systems. The orbital angular momentum of the OH radical becomes fully quenched as it evolves along the $OH+C_2H_2$ reaction coordinate to the HCCHOH radical intermediate, as it is in other chemically bonded free radicals with a single unpaired electron.[13]

The structure of the OH-acetylene complex is expected to closely resemble that of the closed-shell analogs acetylene-HF and acetylene-HCl, which have been studied theoretically as well as experimentally via infrared and microwave methods.[14–21] These closed-shell complexes have T-shaped structures with H*X* (X=F,Cl) forming a hydrogen bond perpendicular to and bisecting the triple bond of acetylene, in which the hydrogen atom of H*X* is closest to the triple bond.[20,21] By contrast, the acetylene-water complex favors a different configuration in which the water molecule acts as a proton acceptor from one of the acetylene hydrogen atoms.[22,23] The configuration in which the water molecule acts as a proton donor to the acetylene triple bond is slightly less favorable and readily converts to the global minimum.[22] Theoretical predictions—from a previous study[5] and the results presented here—indicate that OH-acetylene will be the most stable in a T-shaped structure that is isomorphic with the acetylene-HF and -HCl complexes. A comparison of the structural properties of acetylene complexes with OH, HF, and HCl is included in the discussion.

II. *AB INITIO* CALCULATIONS

Exploratory calculations have been undertaken to investigate the intermolecular potential energy surface (PES) of the OH-acetylene complex. The aim of these calculations is to determine the minimum energy configuration and estimate the binding energy of the complex. In order to provide meaningful results on the OH-acetylene complex from *ab initio* electronic structure calculations, it is necessary to employ a highly correlated treatment such as the restricted coupled cluster singles, doubles, noniterative triples [RCCSD(T)] level of theory. The RCCSD(T) method has been shown to be yield accurate results on other open-shell complexes.[24,25] Furthermore, calculations on weakly bound complexes require a large basis set including diffuse and polarization functions to provide sufficient flexibility to account for the anisotropy of the interaction potential.[26]

In the present work a recently developed extrapolation procedure is adopted to estimate the complete basis set (CBS) limit for the intermolecular PES. The extrapolation procedure has been described in detail elsewhere,[26–28] and has been shown to provide accurate intermolecular energies for a range of chemical species including the N_2-rare gas and OH-Ar complexes.[28] Briefly, *ab initio* calculations are performed for a given geometry of the complex at the restricted Hartree-Fock (RHF) and RCCSD(T) levels of theory using the standard augmented correlation consistent basis set libraries aug-cc-pVDZ and aug-cc-pVTZ of Dunning *et al.*[29–32] The effects of basis set superposition error (BSSE) are then taken into account for each of the calculations by employing the standard Boys-Bernardi counterpoise correction procedure. For a given geometry of the complex the calculations therefore produce a total of four intermolecular energies, E_2^{RHF}, E_2^{cor}, E_3^{RHF}, and E_3^{cor}, corresponding to the

BSSE corrected RHF and correlation energies ($E^{\mathrm{RCCSD(T)}} - E^{\mathrm{RHF}}$) for the two basis set sizes employed. These energies are then extrapolated towards the CBS limit by the use of the expression,

$$E_{\infty}^{\mathrm{tot}} = \frac{3^{\alpha}}{3^{\alpha}-2^{\alpha}} E_3^{\mathrm{RHF}} - \frac{2^{\alpha}}{3^{\alpha}-2^{\alpha}} E_2^{\mathrm{RHF}} + \frac{3^{\beta}}{3^{\beta}-2^{\beta}} E_3^{\mathrm{cor}} - \frac{2^{\beta}}{3^{\beta}-2^{\beta}} E_2^{\mathrm{cor}},$$

where α and β are empirical parameters determined by Truhlar and co-workers ($\alpha=3.4$ and $\beta=2.0$).[33,34]

All *ab initio* calculations were carried out using the MOLPRO 2000.1 software package[35] running on a desktop PC. The OH and acetylene monomers were held at their experimentally determined equilibrium geometries, $r_{\mathrm{O\text{-}H}} = 0.970$ Å, $r_{\mathrm{C\text{-}H}} = 1.061$ Å and $r_{\mathrm{C\text{-}C}} = 1.203$ Å.[36,37] Calculations on the OH-acetylene PES were performed at 11 values of R, the center of mass separation between the two monomers, ranging 2.6–8.0 Å at six different orientations of the OH and acetylene monomers ($\theta_{\mathrm{OH}}, \theta_{\mathrm{C_2H_2}}$), namely, (0,0), (0,90), (90,0), (90,90), (180,0), and (180,90) degrees, with (0,0) corresponding to linear O-H—H-C≡C-H. In all cases the OH and acetylene monomers are constrained to be in the same plane resulting in the complex being described by the C_s point group.

Owing to the $^2\Pi$ symmetry of the ground state of the OH radical, the projection of the electronic orbital angular momentum onto the internuclear axis Λ has two components corresponding to $\Lambda = \pm 1$. In the absence of external fields these two states are degenerate; however, this degeneracy is lifted by the approach of a collision partner resulting in two adiabatic electronic interaction potentials, which split apart from one another in nonlinear configurations. Within the C_s point group these two adiabatic potentials are labeled $^2A'$ or $^2A''$ depending on whether the unpaired electron in the OH radical lies in or out of the plane of the complex, respectively. Separate *ab initio* calculations are conducted for the $^2A'$ and $^2A''$ interaction potentials of the OH-acetylene complex.

Radial cuts of the intermolecular potentials from the extrapolated *ab initio* calculations are shown in Fig. 2 for the (0,90), (90,90), and (180,0) orientations. The cuts for the (0,0) and (180,90) orientations are repulsive at all separation distances and therefore not included. The radial cut in the (90,0) orientation (not shown) is similar to that for (180,0) on the $^2A''$ potential and almost completely repulsive on the $^2A'$ potential. The well depths and corresponding intermolecular distances at specific orientations are summarized in Table I. It is clear from the table that the equilibrium geometry of the OH-acetylene complex corresponds to a T-shaped complex ($\theta_{\mathrm{OH}}, \theta_{\mathrm{C_2H_2}}$) = (0,90) with the H of OH pointing towards the C≡C bond of the acetylene unit. Thus, the OH radical acts as a proton donor to the acetylene triple bond. The dissociation energy D_e of the complex in this configuration is calculated to be 1132 cm^{-1} on the $^2A''$ surface and 987 cm^{-1} on the $^2A'$ surface using the extrapolation procedure. For comparison, RCCSD(T) calculations performed using the aug-cc-pVDZ and aug-cc-pVTZ basis sets, but without using the extrapolation procedure, yield dissociation energies at the (0,90) orientation of 803 and 991 cm^{-1}, respectively, on the $^2A''$ surface. In addition, the present CBS results supersede the much older calculations of Sosa and Schlegel.[5]

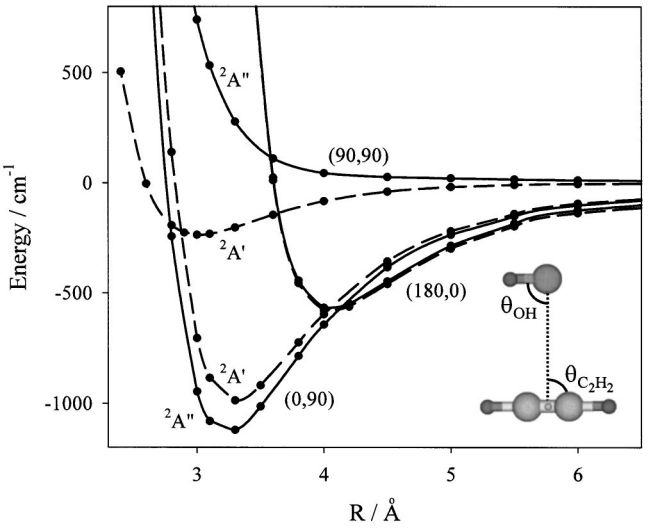

FIG. 2. Radial cuts (smoothed curves) of the OH+C_2H_2 intermolecular potential surface for fixed orientations of the monomers ($\theta_{\mathrm{OH}}, \theta_{\mathrm{C_2H_2}}$) = (0,90), (90,90), and (180,0) degrees. The *ab initio* calculations were carried out at the distances indicated by data points using the RCCSD(T) level of theory with an extrapolation procedure to estimate the complete basis set limit. The equilibrium geometry of the OH-acetylene complex is the T-shaped (0,90) configuration. The $^2A'$ and $^2A''$ surfaces (dashed and solid lines) correspond to the half-filled $p\pi$ orbital of the OH radical lying perpendicular or within the plane of the complex, respectively.

The separation between the $^2A''$ and $^2A'$ surfaces increases with decreasing separation distance in nonlinear configurations, reaching a magnitude of ~140 cm^{-1} at the equilibrium T-shaped geometry, which is comparable to the spin-orbit splitting of OH.[38] This large energy difference has significant ramifications on the intermolecular energy level structure of the OH-acetylene complex that are discussed in a related theory paper.[12]

Shallow wells were found at longer intermolecular distances for configurations with acetylene acting as the proton donor and OH as the acceptor, namely, the linear HO-HCCH configuration at (180,0) and the L-shaped configuration with the O of OH interacting with a hydrogen atom of acetylene at (90,0). In the L-shaped configuration, the attractive interaction is stronger for the $^2A''$ surface with its half-filled $p\pi$ orbital perpendicular to the nuclear plane. The true secondary minimum likely lies intermediate between these two orientations, as found for acetylene-HF.[15] Finally, an intriguing local minimum is found on the $^2A'$ surface in the (90,90) configuration at $R = 3.0$ Å that may reflect the start of chemical bonding with the OH radical oriented appropriately for addition to the C≡C bond. This configuration looks similar to TS1 (Fig. 1), but is constrained by fixed monomer bond lengths and linear structures in the calculations and therefore cannot evolve fully to TS1.

TABLE I. Comparison of well depths (D_e) and intermolecular distances (R_e) for specific orientations of the OH-C_2H_2 complex in its ground electronic state calculated at the RCCSD(T) level of theory using the basis set extrapolation procedure described in the text.

$(\theta_{OH}, \theta_{C_2H_2})$	(0,90)		(180,0)	(90,0)		(90,90)	
	$^2A'$	$^2A''$	$^2\Pi$	$^2A'$	$^2A''$	$^2A'$	$^2A''$
R_e/Å	3.29	3.23	4.05	4.18	4.07	3.02	···[a]
D_e/cm^{-1}	987.3	1131.7	570.4	91.8	496.0	236.2	···[a]

[a]The $^2A''$ surface is repulsive in the (90,90) orientation.

III. EXPERIMENT

The infrared action spectrum of the OH-acetylene reactant complex and the OH product state distribution resulting from vibrational predissociation have been recorded by an IR pump–UV probe technique.[39,40] The IR pump laser excites the OH-acetylene reactant complex in the OH overtone region ($v=2\leftarrow0$), and the UV probe laser detects the OH ($v=1$) fragments by saturated laser-induced fluorescence (LIF) in the OH $A\,^2\Sigma^+ - X\,^2\Pi(0,1)$ region. The IR pump laser is scanned to obtain the infrared action spectrum; alternatively, the UV probe laser is scanned through various OH transitions to determine the primary product channels.

Binary complexes composed of the OH and C_2H_2 reactants are produced using the following procedure. Acetylene is passed through an activated charcoal filter and mixed with Ar to prepare 5%–10% acetylene mixtures in a 4 L stainless steel cylinder. This carrier gas mixture (at a delivery pressure of 60 psi) flows over a 90 wt % nitric acid sample to entrain its vapor and is pulsed into a vacuum chamber. Hydroxyl radicals are produced by 193 nm photolysis of HNO_3 near the exit of a quartz capillary tube (ID=1 mm) that is affixed to the pulsed valve. Collisions between the photolytically generated OH radicals and carrier gas in the early stages of the supersonic expansion result in chemical reaction, cooling of OH, and/or OH-acetylene complex formation.

Acetylene is also photolyzed at 193 nm[41,42] although its absorption cross section is much smaller than that for HNO_3.[43] Using the absorption cross sections,[42,43] quantum yields,[41,44,45] and concentrations in the gas mixture, we estimate that an order of magnitude more OH radicals are produced for every acetylene molecule photolyzed, making this a minor process in the production of OH-acetylene complexes. We observe no evidence of acetylene photolysis in these experiments.

Tunable infrared radiation at $\sim$1.4 μm is generated by an optical parametric oscillator (Laservision custom OPO, 0.15 cm^{-1} linewidth) pumped by an injection-seeded Nd:YAG laser (Continuum Precision II 8000; 8 ns pulse, 10 Hz repetition rate). The OPO delivers up to 16–18 mJ/pulse of IR radiation in the interaction region. The absolute frequency of the OPO is determined by recording an H_2O photoacoustic spectrum as the infrared laser is scanned, and comparing to well-documented $H_2O\,(2,0^0,0)$ transitions.[46] Relative frequency markers were also obtained with an etalon (FSR=0.343 cm^{-1}).

The UV probe beam was generated by the frequency doubled output of a Nd:YAG pumped dye laser (Quantel 581, Continuum ND 6000, 20 Hz) operating with LDS 698 dye, which produced tunable radiation around 348 nm. Typically, $\sim$1 mJ pulse of UV radiation was passed into the vacuum chamber. The UV laser was calibrated using the well-known frequencies of the OH A-$X(0,1)$ lines.[47,48]

The IR and UV laser beams were counterpropagated, focused, and spatially overlapped in the vacuum chamber $\approx$15 mm downstream from the exit of the capillary. The focused beams in the interaction region measure $\approx$1 mm^2. The resultant LIF signal is collected with $f/1$ optics and detected using a blue sensitive photomultiplier tube (PMT, EMI 9813Q) positioned perpendicular to both the supersonic jet and laser axes. Several filters and a PMT gating circuit were used to block scattered light arising from the photolysis and UV probe lasers, while still passing the desired fluorescence in the OH A-$X(0,0)$ spectral region. The LIF signal detected at the PMT was preamplified, integrated with a boxcar, and transferred to a computer for processing. The lasers were synchronized such that the IR pump laser (10 Hz) was present for every other UV probe laser pulse (20 Hz), with the UV laser pulse typically delayed from the IR pulse by 50 ns. An active subtraction technique was used in processing the data in order to subtract the background signal observed with the UV laser alone from the infrared-induced signal obtained with both IR and UV lasers present. The background signal arises from incomplete cooling of uncomplexed OH in the supersonic expansion. Typically, the LIF signal arising from 150 laser shots (75 IR+UV, 75 UV only) was collected and averaged for each data point.

IV. RESULTS AND ANALYSIS

A. Infrared spectrum

A spectroscopic search in the vicinity of the OH overtone transition revealed a new feature at 6885.5 cm^{-1}, shifted 85.8 cm^{-1} to lower energy of free OH, when acetylene was introduced to the carrier gas. The rotational band structure associated with this feature is shown in Fig. 3; several scans were averaged to obtain the figure. This infrared action spectrum was recorded with the UV probe laser fixed on the OH A-$X(0,1)\,Q_1(11)$ transition, which was empirically found to give the strongest infrared-induced signal and the best signal-to-background ratio. The rotational band structure is consistent with the assignment of this transition as the OH overtone stretch ($2\nu_{OH}$) of the OH-acetylene reactant complex as detailed below.

The rotational band structure is characteristic of a parallel (a-type) transition of a near prolate asymmetric top, exhibiting simple PQR band structure with an unresolved cen-

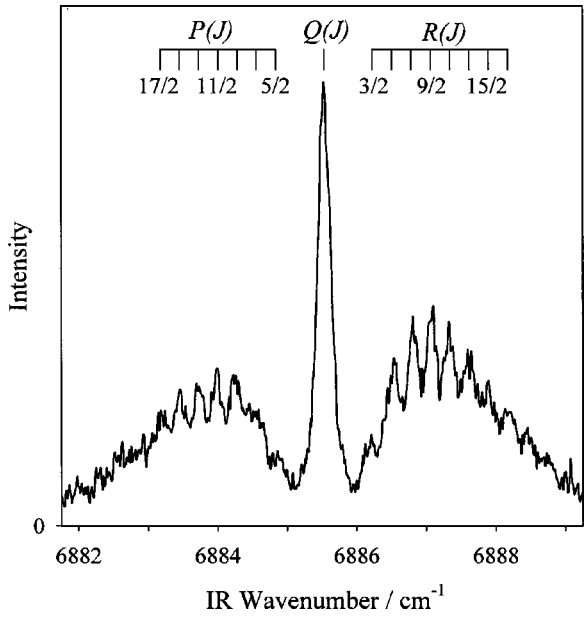

FIG. 3. Rotationally resolved infrared action spectrum of the OH overtone band of the OH-acetylene reactant complex at 6885.5 cm^{-1} (band origin). The rotational structure is indicative of a parallel (*a*-type) transition of a near prolate asymmetric top. The appearance of *P* and *R* lines at *odd* multiples of $(B+C)/2$ with respect to the central *Q* branch indicates that the spin of the OH radical is coupled to the molecular frame. The ticks show calculated line positions for those lines included in the fit.

tral *Q* branch and partially resolved *P* and *R* branches. The transition type indicates that the OH subunit lies along the *a*-inertial axis, as expected for a T-shaped complex in which OH is hydrogen-bonded to the π cloud of acetylene, $(\theta_{OH}, \theta_{C_2H_2}) = (0,90)$. Similar band structure has previously been reported at much higher resolution for the fundamental H*X* (*X*=F or Cl) stretches of the acetylene-HF and acetylene-HCl complexes.[14,19] The large spectral shift suggests that the OH subunit is significantly perturbed upon forming a hydrogen bond with the H side of OH interacting with acetylene.

The lines in the *P* and *R* branches are uniformly spaced by $\sim(B+C)$, but at *odd* multiples of $(B+C)/2$ relative to *Q* branch, rather than the *even* multiples seen for other acetylene-H*X* complexes.[14,19] The *odd* multiples with respect to the central *Q* branch are a direct consequence of the half-integral values of the total angular momentum *J* in the complex, which arises when the spin associated with the unpaired electron of the OH radical is coupled to the molecular frame.[49] The ticks in Fig. 3 represent the calculated line positions derived from a least squares fit that was performed by varying the lower and upper state values of the $(B+C)/2$ rotational constant and band origin (ν_0) for an assumed near prolate asymmetric top. Ticks are shown only for those rotational lines that were included in the fit. Spectroscopic constants determined from this fit are given in Table II. The complex undergoes no discernable change in the $(B+C)/2$ rotational constant upon OH overtone excitation. The present experiments lack the spectral resolution required to measure the asymmetry splitting or determine the *A* rotational constant. However, we can assume that the *A* constant will be essentially that of the *B* value of free C_2H_2 ($B = 1.176608\,cm^{-1}$),[50] as found in the previously investigated closed shell systems.[14,19–21]

TABLE II. Spectroscopic constants and structural parameters of OH-acetylene, acetylene-HF, and acetylene-HCl complexes.

	OH-acetylene overtone[a]	Acetylene-HF fundamental	Acetylene-$H^{35}Cl$ fundamental
ν_0 (cm^{-1})	6885.53(1)	3794.365[b]	2806.9172[c]
Spectral shift (cm^{-1})	−85.81(1)	−167.202	−79.0605
$\frac{1}{2}(B''+C'')$ (cm^{-1})	0.1388(4)[d]	0.1478080[e]	0.0798830[f]
$\frac{1}{2}(B'+C')$ (cm^{-1})	0.1388(4)[d]	0.15109[b]	0.081265[c]
R_{cm} (Å)	3.327(5)	3.075[e]	3.663[f]
$R(X-*)$ (Å)[g]	3.385(5)	3.122	3.699
D_0 (cm^{-1})	<956	1088(2)[h]	830(6)[i]

[a]This work.
[b]Reference 19.
[c]Reference 14.
[d]1σ uncertainty from fit.
[e]Reference 20.
[f]Reference 21.
[g]$R(X-*)$ is the distance between the heavy atom (O, F, or Cl) and the center of the C≡C bond.
[h]Reference 17.
[i]Reference 18.

The separation between the centers-of-mass of the OH and C_2H_2 partners can be evaluated from the rotational constants assuming that the monomer units are unchanged upon complex formation. The values determined are 3.327(5) Å for the both the ground and excited vibrational states. The ground state separation derived experimentally, $R_0 = 3.327(5)$ Å, is slightly larger, as expected, than that predicted theoretically for the T-shaped minimum energy configurations, $R_e = 3.23$ and 3.29 Å, on the $^2A''$ and $^2A'$ surface (see Table I). The zero-point motion of the complex will sample both of these surfaces. By contrast, it appears to be incompatible with a linear HO-HCCH structure, $(\theta_{OH}, \theta_{C_2H_2}) = (180,0)$ with OH acting as a proton acceptor, which is predicted to have a strongly repulsive interaction at this separation distance (see Fig. 2).

B. OH product state distribution

The quantum state distribution of the OH fragments resulting from vibrational predissociation of the OH-acetylene $(2\nu_{OH})$ complex has also been examined. The release of one quantum of OH vibrational excitation is sufficient to break the intermolecular bond and cause fragmentation of the complex into OH $(v=1)$ and C_2H_2 products; a propensity for the loss of one quantum of OH vibrational excitation has been observed previously.[40] The relative population of the OH $(v=1)$ products is derived from the intensities of Q_1 branch lines as the UV laser is scanned through the OH A-$X(0,1)$ transition following infrared excitation of the OH-acetylene complex at 6885.5 cm^{-1}. The line intensities were scaled relative to the $Q_1(11)$ line, which was scanned immediately before and after every other line to account for variations in the experimental conditions. The intensities of lines in other branches, namely, Q_2, P_1, and P_2, were much smaller than the corresponding Q_1 line due to fine structure propensities.[40] Measurement of transition intensities was per-

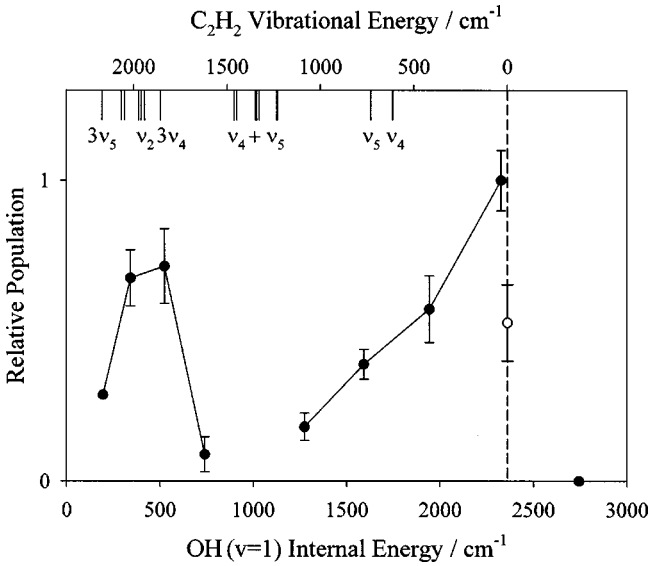

FIG. 4. The OH ($v=1$) product state distribution and associated internal energy resulting from vibrational predissociation of OH-acetylene ($2\nu_{OH}$). The OH fragment distribution peaks at $j_{OH}=23/2$ in the lower ($\omega=3/2$) spin-orbit manifold (filled symbols) and a secondary maximum is seen at $j_{OH}=11/2$, $\omega=3/2$. No population is observed in product states higher than $j_{OH}>21/2$ in the excited ($\omega=1/2$) spin-orbit manifold (open circle), setting an upper limit for the OH-acetylene binding energy of $D_0\leqslant 956\ \mathrm{cm}^{-1}$ (dashed line). Certain product states, namely, $j_{OH}=3/2$, 5/2, and 15/2 ($\omega=3/2$), could not be measured as discussed in the text. The ticks at the top of the figure indicate energetic limits for producing OH ($v=1$) with vibrationally excited acetylene cofragments denoted by the labels.

formed in the fully saturated LIF regime and appropriately converted into relative populations of OH ($v=1$) rotational levels.[51,52]

The resultant population distribution of OH ($v=1,j_{OH}$) fragments in the ground $\omega=3/2$ spin-orbit manifold is shown in Fig. 4. The distribution peaks in a highly rotationally excited state, $j_{OH}=23/2$, with 2325 cm^{-1} of rotational energy. A secondary maximum is observed for the $j_{OH}=9/2$ and 11/2 states with 343 and 524 cm^{-1} of energy, respectively. Noticeably less population is observed in other rotational states, including the intervening states between the primary and secondary maxima, and thus we characterize the OH product state distribution as bimodal. The population in the lowest OH ($v=1$) rotational levels, $j_{OH}=3/2$ and 5/2, could not be measured due to large background population in these levels. In addition, the population of the $j_{OH}=15/2$ state could not be determined due to an overlapping OH-Ar feature at the OH A-$X(0,1)$ $Q_1(7)$ probe frequency. The abrupt cut off beyond $j_{OH}=23/2$, $\omega=3/2$ was examined in more detail by probing the $j_{OH}=21/2$ level of the excited spin-orbit manifold ($\omega=1/2$) at 2361 cm^{-1} using the $Q_2(10)$ line, which is populated in the dissociation process, and the next higher state, $j_{OH}=25/2$, $\omega=3/2$, at 2741 cm^{-1}, which appears to be closed.

The highest energetically open OH ($v=1$) product state, $j_{OH}=21/2$, $\omega=1/2$, leaves less than 956 cm^{-1} of energy available for breaking the OH-acetylene intermolecular bond (D_0), internal excitation of the C_2H_2 fragment (v,j), and translational recoil of the fragments (E_{trans}), as illustrated in the following energy cycle:

$$\mathrm{OH\text{-}C_2H_2}(2\nu_{OH}) - D_0 \rightarrow \mathrm{OH}(v=1, j_{OH}) + \mathrm{C_2H_2}(v,j) + E_{trans}.$$

This provides an upper limit for the ground state binding energy of the OH-acetylene complex of $D_0\leqslant 956\ \mathrm{cm}^{-1}$. This calculation neglects internal excitation of the correlated C_2H_2 product and translational recoil, the latter expected to be small based on energy gap arguments,[53] which would lower the limiting value. Vibrational excitation of the correlated C_2H_2 fragment seems unlikely since excitation of even the lowest frequency bending modes, 613 and 730 cm^{-1},[54] would lead to an unreasonably small D_0. Thus, the highly rotationally excited OH ($v=1$) products are accompanied by acetylene cofragments in their ground vibrational state, indicating that vibrational predissociation proceeds by a vibration to rotation and/or translation (V-R,T) energy transfer process. Rotational excitation of the acetylene fragment is expected to be small by analogy with prior results on acetylene-HF,[17] where only the lowest two rotational states were populated, as well as the fact that its small rotational constant prevents this degree of freedom from accommodating much energy.

The bimodal product state distribution suggests that more than one mechanism may be operative in the vibrational predissociation dynamics, as found previously in systems such as HF-acetylene and OH-CO.[17,40,55] The secondary peak in the OH ($v=1$) rotational distribution at lower energy likely arises from vibrational excitation of the C_2H_2 cofragment in a vibration-to-vibration (V-V) energy transfer process, which would leave less energy available for rotational excitation of OH ($v=1$). Possible vibrational states and associated energies of the C_2H_2 fragment[54] are shown along the top axis of Fig. 4. For example, the secondary channel that produces OH ($v=1$, $j_{OH}=9/2$, 11/2) is likely to be associated with C_2H_2 products with one quantum of C≡C stretch (ν_2) excitation or three quanta of bend ($3\nu_4$, $3\nu_5$, or combinations of these modes). These C_2H_2 product states may be preferred from the point of view of closer vibrational resonance, even though a large number of quanta would need to be changed to access the bending states.[56]

Finally, the lifetime of the vibrationally activated OH-acetylene reactant complex due to inelastic (vibrational predissociation) and/or reactive decay was examined through time- and frequency-domain measurements. Varying the IR pump–UV probe delay time showed that the appearance of OH ($v=1$) fragments was controlled by the temporal duration of the IR laser pulse, indicating a lifetime of less than 8 ns. In addition, the linewidth of the infrared spectrum (Fig. 3) has been fitted using a model developed in a related theory paper to simulate its rotational band structure.[12] If the OH radical's orbital angular momentum is unquenched, then the spectrum is best fit with a linewidth of 0.19 cm^{-1}. This is slightly larger than the laser bandwidth (0.15 cm^{-1}), suggesting the possibility of homogeneous broadening due to either lifetime or power broadening. (Unfortunately, the signal-to-noise level of the P and R branches was not adequate to test the effect of IR laser power on the linewidth.) However, model calculations indicate a more likely alternate explanation of inhomogeneous line broadening for the apparent

broadening.[12] If the OH radical's orbital angular momentum is partially quenched, as expected, then the spectrum can be fit with a laser-limited linewidth of 0.15 cm^{-1}. See the theory paper for details on the fit and simulations.[12]

V. DISCUSSION

As discussed in the *ab initio* calculation section, the nonlinear configuration of the OH-acetylene complex results in a lifting of the OH monomer electronic orbital degeneracy into $^2A'$ and $^2A''$ electronic states. For previously studied OH-containing complexes such as OH-Ar (Ref. 57) and OH-H_2,[58] this separation, known as the difference potential, is sufficiently small that the OH radical's orbital degeneracy is approximately retained in a zeroth-order description of the rotational motion of the complex. The appropriate quantum numbers are the half-integer total angular momentum J, which is a rigorously good quantum number, irrespective of the magnitude of the difference potential, the projection P of J on the a inertial axis of the complex, and $\omega=\lambda+\sigma$, the sum of the projections of the electronic orbital and spin angular momenta, respectively, along the OH, monomer axis. The effects of the difference potential can then be included, if necessary, via perturbation theory.[59]

For the somewhat more strongly bound complexes of OH with N_2 (Ref. 60) or CO,[39,55] the linear equilibrium geometry preserves the cylindrical symmetry of the OH monomer upon complex formation so that the electronic degeneracy persists at this configuration. Although the degeneracy is lifted by bending vibrations that sample nonlinear geometries, the molecular wave functions still reflect the underlying symmetry of the Hamiltonian, and are labeled by the same quantum numbers as above. The effects of the difference potential are included in the Renner-Teller effect,[61,62] so that the unquenched electronic angular momentum is included in the vibronic state of the molecule, for which rotational energy levels can then be determined.[63]

OH-acetylene is more strongly bound than these previously studied complexes, and the *ab initio* calculations show that the magnitude of the difference potential at the T-shaped equilibrium geometry (140 cm^{-1}) is comparable to the spin-orbit splitting for free OH. As discussed elsewhere,[12] the difference potential is large enough that perturbation theory will not be sufficient to account for the effects of the $^2A'-^2A''$ splitting. Nevertheless, the form of the OH overtone spectrum for OH-acetylene, with P- and R-branch lines at *odd* multiples of $(B+C)/2$ relative to Q branch, indicates that this complex retains sufficient unquenched electronic orbital angular momentum to keep the spin of the unpaired electron coupled to the molecular framework.[48] Thus, the small difference potential limit, and the quantum numbers J, P, and ω, as used in the more weakly bound complexes, are appropriate in discussing the spectrum. Two experimental considerations, the rotational temperature in the jet expansion and the laser line width, work together with the a-type dipole selection rules to hide the effects of the difference potential.

In fact, model calculations[12] predict that the qualitative appearance of an a-type band with unresolved sub-band structure and rotational temperatures of ~10 K will be independent of the precise value of the difference potential for moderate energy differences between the $^2A'$ and $^2A''$ states, up to approximately the OH monomer spin-orbit splitting. This is not surprising since an a-type transition occurs with no change in the component of angular momentum about the a inertial axis. Thus, the spectrum is relatively insensitive to the changes in rotational motion about this axis caused by the $^2A'-^2A''$ splitting. The difference potential does cause significant parity splitting of rotational levels with $P=\pm 1/2$, $\omega=\pm 3/2$, similar to that seen previously for corresponding levels in OH-Ar,[59,64] OH-CO,[39] and OH-N_2.[60] At the present experimental resolution and rotational temperature, however, these lines are buried under the wings of the more numerous, less strongly affected lines, and contribute only to inhomogeneous line broadening.

Interestingly, the model calculations also indicate that the effects of inertial asymmetry are reduced even at the moderate difference potential appropriate to OH-acetylene. Thus, the rotational structure of the OH stretching overtone, a-type band will even more closely resemble that of a symmetric top than might be otherwise expected. The OH overtone spectrum can then be analyzed as if it were a parallel transition of a symmetric top with overlapping sub-bands and half-integer values for the rotational quantum numbers. Only the spectroscopic constant $(B+C)/2$ may be obtained from the analysis, as the spectrum provides no measurable information regarding the value of $B-C$.

In a related theory paper,[12] we consider whether a better zero-order description of the rotational motion might be the limit where the electronic orbital angular momentum is fully quenched in the OH-acetylene complex. This is precisely the limit for the more familiar case of a chemically bonded, asymmetric top molecule with a single unpaired electron.[13] The spin of the unpaired electron is decoupled from the molecular framework, and the rotational energy levels in this case are labeled with familiar integer, asymmetric top quantum numbers $N_{K_aK_c}$. At moderate resolution in this limit with unresolved K structure, the a-type vibrational spectrum for a near-prolate asymmetric top, such as OH-acetylene, would still resemble a parallel band of a symmetric top, but one characterized by *integer* rotational quantum numbers. In particular, it would have a prominent Q branch at the band origin and lines in the P and R branches would appear at *even* multiples of $(B+C)/2$ on either side. Clearly, the observed OH overtone band of OH-acetylene is better described in the small difference potential limit, which is used in the rotational analysis presented here.

The rotational analysis yields $(B+C)/2$ and the associated separation distance between the centers of mass of OH and acetylene of 3.327(5) Å at the zero-point level. This compares favorably with the separation distance at the T-shaped equilibrium configuration obtained from *ab initio* calculations presented here, as would be expected given the high level of theory, RCCSD(T), and basis set extrapolation procedure used in the calculations. The OH-acetylene bond length is found to be intermediate between those previously observed for acetylene-HF and acetylene-HCl,[20,21] as shown in Table II, reflecting the general trend in magnitude of the HX dipole moments.

The separation between the OH and acetylene subunits is essentially unchanged when the OH-acetylene complex is vibrationally excited in the OH stretching mode. This differs from acetylene-HF and -HCl complexes,[14,19] where a *decrease* in intermolecular bond length was observed upon H*X* excitation. This decrease can be attributed to an increase in the dipole moment of the HX monomer and an associated increase in the strength of the electrostatic interaction. In addition, the spectral shift associated with the OH overtone transition, while large for OH complexes studied to date is much less than seen for the fundamental HF vibration of acetylene-HF and comparable to that for the fundamental HCl vibration of acetylene-HCl. Typically, the shift of an overtone transition is twice that of a fundamental transition, so the spectral shift of the OH overtone transition of OH-acetylene appears to be anomalously small. The spectral shift reflects the increased strength of the intermolecular interaction upon vibrational excitation of the H*X* monomer. The unusual behavior in spectral shift and bond length changes for OH-acetylene is likely caused by the atypical dipole moment function for OH,[65,66] which is approaching its maximum value at internuclear distances contained between the classical turning points for $v=2$. Thus, the OH dipole moment does not increase as much as would be expected with a linear dipole function, resulting in smaller changes in the electrostatic interaction between OH $(v=0)$ and $(v=2)$ with the acetylene partner.

The vibrational predissociation dynamics of the OH-acetylene complex prepared with two quanta of OH stretch is summarized in Fig. 5. The left column shows the OH overtone excitation step and energy available to fragments, $\nu_0 - D_0$, the right column shows the OH $X\,^2\Pi_{3/2}(v=1,j_{\mathrm{OH}})$ product rotational states that are energetically open, and the middle column shows the energetically allowed vibrational states of the acetylene fragment.[54] The highest energetically open OH $(v=1)$ product state, $j_{\mathrm{OH}}=21/2$, $\omega=1/2$, provides an upper limit for the binding energy of the OH-acetylene complex in its ground state, $D_0 \leqslant 956\,\mathrm{cm}^{-1}$. The strength of the OH-acetylene interaction is intermediate between acetylene-HF and acetylene-HCl (see Table II), in accord with the relative magnitudes of the H*X* dipoles. The most populated $X\,^2\Pi_{3/2}$ $(v=1,j_{\mathrm{OH}})$ product states are highlighted in Fig. 5 with the width of the line roughly proportional to their population. Population of the $j_{\mathrm{OH}}=23/2$ and 21/2 states does not leave sufficient energy to vibrationally excite acetylene, and thus the dominant predissociation process must occur by a *V-R, T* mechanism. The other significantly populated states, $j_{\mathrm{OH}}=11/2$ and 9/2, are consistent with a *V-V* mechanism. The acetylene ν_2 C≡C stretch and three quanta of bend, e.g., $3\nu_4$, $2\nu_4+\nu_5$, or $3\nu_5$, are possible acceptor modes.[54] The latter may be less favorable due to the large number of quanta that must be changed.[56] Both *V-V* and *V-R, T* energy transfer processes were observed following fundamental HF excitation of the acetylene-HF complex,[17] however, only one quantum of acetylene bend, ν_4 or ν_5, was energetically accessible. For other OH complexes, *V-V* energy transfer is the dominant predissociation mechanism in the OH-CO complex,[40] and is seen exclusively in the OH-N_2 and OH-CH_4 complexes.[60,67]

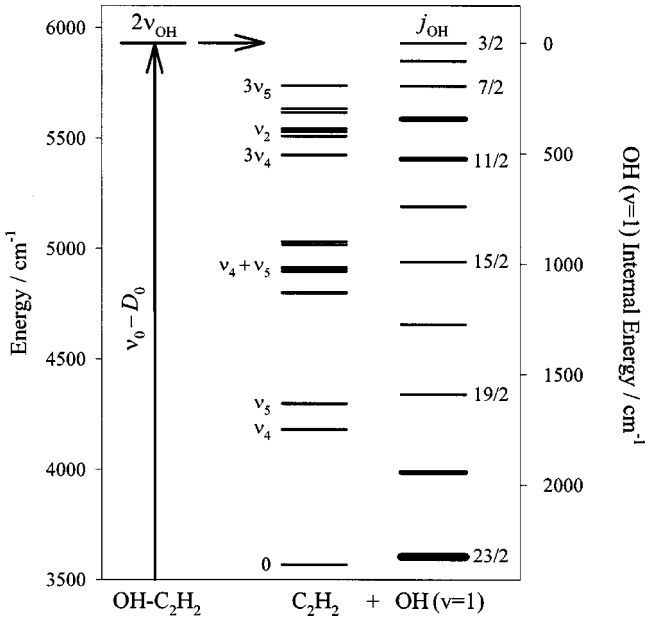

FIG. 5. Energy level diagram illustrating the inelastic scattering dynamics of OH-acetylene reactant complexes prepared with two quanta of OH stretch. The arrow on the left-hand side indicates the total energy available to the fragments, $\nu_0 - D_0$, with zero of energy defined as the OH $X\,^2\Pi_{3/2}(v=0,j=3/2)+C_2H_2$ asymptote. The central region shows the energetically allowed vibrational states of inelastically scattered C_2H_2 fragments correlating with OH $(v=1)$. The right-hand side illustrates the allowed rotational levels (j_{OH}) of OH $(v=1)$ fragments in the $\omega=3/2$ spin-orbit manifold and associated internal energy, as discussed in the text. The most populated OH rotational states are highlighted.

The present experiment does not probe reaction products, only inelastically scattered OH fragments. The transition state for the addition reaction requires internal rotation of the OH subunit,[5] as shown in Fig. 1. Combination bands that might access excited bending states involving the OH moiety have not yet been observed by infrared action spectroscopy, at least not when probing the OH fragments of vibrational predissociation.

VI. CONCLUSIONS

A weakly bound complex between the OH and acetylene reactants has been stabilized in a supersonic expansion, characterized using an IR pump–UV probe method, and also investigated by high level *ab initio* calculations. Analysis of the *a*-type rotational band structure associated with the OH overtone transition at 6885.5 cm^{-1} (origin) is consistent with the T-shaped minimum energy configuration predicted by theory. The spectrum of the near prolate asymmetric top reveals half-integral values of the total angular momentum, arising from the spin of the unpaired electron of OH being coupled to the molecular frame. A slight broadening in the OH overtone spectrum is suggestive of inhomogeneous broadening due to partial quenching of the OH radical's orbital angular momentum.[12] This partial quenching is clearly observed in spectra recorded in the asymmetric acetylenic stretch region that will be presented in a future publication.[11] Our success in isolating the OH-acetylene reactant complex, which has only a small barrier to reaction, indicates that it

may be possible to stabilize complexes composed of other reactive species, such as OH radicals with aliphatic and aromatic π systems.

The stability of the OH-acetylene reactant complex is determined from the highest observed OH ($v=1$) product state, namely, $j_{OH}=21/2$, $\omega=1/2$, which can be detected by laser-induced fluorescence. This establishes a firm upper limit of 956 cm^{-1} for the ground state binding energy (D_0) of the complex. This value is in good accord with the equilibrium dissociation energy, $D_e=1131\,cm^{-1}$ ($^2A''$), obtained at the RCCSD(T) level of theory with extrapolation to the complete basis set limit. A comprehensive mapping of populated OH $X\,^2\Pi_{3/2}(v=1,j_{OH})$ product states reveals that vibrational predissociation occurs primarily by intramolecular vibrational to rotational energy transfer and secondarily through intermolecular vibrational energy transfer to specific bend and/or stretch modes of acetylene. Future experiments will attempt to detect reaction products, in addition to the inelastically scattered OH fragments detected in the present work. The hydrogen-bonded OH-acetylene complex characterized in this study may play a role in the initial addition of OH to acetylene, as suggested in the related OH-ethylene system.[6–9] However, dynamical calculations, analogous to those carried out for OH-CO,[68,69] are still needed to ascertain the exact role of the reactant channel well in the electrophilic addition of OH to acetylene under thermal conditions.

ACKNOWLEDGMENTS

This research was sponsored by the Office of Basic Energy Sciences of the Department of Energy. M.D.M. thanks the H. Axel Schupf '57 Fund for Intellectual Life at Amherst College for sabbatical leave support. M.D.W. acknowledges support from the ARF program of the EPSRC for providing the computational facilities upon which this study was conducted.

[1] B. J. Finlayson-Pitts and J. N. Pitts, Jr., *Chemistry of the Upper and Lower Atmosphere* (Academic, San Diego, 2000).
[2] D. D. Davis, S. Fischer, R. Schiff, R. T. Watson, and W. A. Bolinger, J. Chem. Phys. **63**, 1707 (1975).
[3] *Kinetics and Mechanisms of the Gas-Phase Reactions of the Hydroxyl Radical with Organic Compounds*, edited by R. Atkinson (AIP, New York, 1989), Vol. Monograph No. 1.
[4] J. V. Michael, D. F. Nava, R. P. Borkowski, W. A. Payne, and I. J. Stief, J. Chem. Phys. **73**, 6108 (1980).
[5] C. Sosa and H. B. Schlegel, J. Am. Chem. Soc. **109**, 4193 (1987).
[6] S. M. Kathmann, M. Dupuis, and B. C. Garrett (private communication).
[7] J. R. Alvarez-Idaboy, N. Mora-Diez, and A. Vivier-Bunge, J. Am. Chem. Soc. **122**, 3715 (2000).
[8] M. Mozurkewich and S. W. Benson, J. Phys. Chem. **88**, 6429 (1984).
[9] D. L. Singleton and R. J. Cvetanovic, J. Am. Chem. Soc. **98**, 6812 (1976).
[10] Y.-H. Ding, X. Zhang, Z.-S. Li, X.-R. Huang, and C.-C. Sun, J. Phys. Chem. A **105**, 8206 (2001).
[11] M. D. Marshall, J. B. Davey, M. E. Greenslade, and M. I. Lester J. Chem. Phys. (to be published).
[12] M. D. Marshall and M. I. Lester, J. Chem. Phys. **121**, 3019 (2004), following paper.
[13] I. C. Bowater, J. M. Brown, and A. Carrington, Proc. R. Soc. London, Ser. A **333**, 265 (1973).
[14] P. Carcabal, M. Broquier, M. Chevalier, A. Picard-Bersellini, V. Brenner, and P. Millie, J. Chem. Phys. **113**, 4876 (2000).
[15] G. E. Douberly, K. Nauta, and R. E. Miller, Chem. Phys. Lett. **377**, 384 (2003).
[16] L. Oudejans and R. E. Miller, Annu. Rev. Phys. Chem. **52**, 607 (2001).
[17] L. Oudejans, D. T. Moore, and R. E. Miller, J. Chem. Phys. **110**, 209 (1999).
[18] L. Oudejans and R. E. Miller, J. Phys. Chem. A **103**, 4791 (1999).
[19] Z. S. Huang and R. E. Miller, J. Chem. Phys. **86**, 6059 (1987).
[20] W. G. Read and W. H. Flygare, J. Chem. Phys. **76**, 2238 (1982).
[21] A. C. Legon, P. D. Aldrich, and W. H. Flygare, J. Chem. Phys. **75**, 625 (1981).
[22] D. Tzeli, A. Mavridis, and S. S. Xantheas, J. Chem. Phys. **112**, 6178 (2000).
[23] P. A. Block, M. D. Marshall, L. G. Pedersen, and R. E. Miller, J. Chem. Phys. **96**, 7321 (1992).
[24] G. C. Groenenboom and N. Balakrishnan, J. Chem. Phys. **118**, 7380 (2003).
[25] G. C. Groenenboom and I. M. Struniewicz, J. Chem. Phys. **113**, 9562 (2000).
[26] P. R. Butler and A. M. Ellis, Mol. Phys. **99**, 525 (2001).
[27] M. D. Wheeler and A. M. Ellis, Chem. Phys. Lett. **374**, 392 (2003).
[28] K. Patel, P. R. Butler, A. M. Ellis, and M. D. Wheeler, J. Chem. Phys. **119**, 909 (2003).
[29] T. H. Dunning, Jr., J. Chem. Phys. **90**, 1007 (1989).
[30] D. E. Woon and T. H. Dunning, Jr., J. Chem. Phys. **98**, 1358 (1993).
[31] D. E. Woon and T. H. Dunning, Jr., J. Chem. Phys. **100**, 2975 (1994).
[32] A. K. Wilson, D. E. Woon, K. A. Peterson, and T. H. Dunning, Jr., J. Chem. Phys. **110**, 7667 (1999).
[33] D. G. Truhlar, Chem. Phys. Lett. **294**, 45 (1998).
[34] P. L. Fast, M. L. Sanchez, and D. G. Truhlar, J. Chem. Phys. **111**, 2921 (1999).
[35] MOLPRO, A package of *ab initio* programs designed by H.-J. Werner and P. J. Knowles, version 2002.1 (2002).
[36] K. P. Huber and G. Herzberg, *Constants of Diatomic Molecules* (data prepared by J. W. Gallagher and R. D. Johnson III) in NIST Chemistry WebBook, NIST Standard Reference Database Number 69, edited by P. J. Linstrom and W. G. Mallard (National Institute of Standards and Technology, Gaithersburg, MD, 2003), 20899. (http://webbook.nist.gov).
[37] CRC, *Handbook of Chemistry and Physics*, 2nd electronic ed. (CRC, Boca Raton, Fla., 1999).
[38] J. A. Coxon, Can. J. Phys. **58**, 933 (1980).
[39] M. D. Marshall, B. V. Pond, and M. I. Lester, J. Chem. Phys. **118**, 1196 (2003).
[40] B. V. Pond and M. I. Lester, J. Chem. Phys. **118**, 2223 (2003).
[41] A. Lauter, K. S. Lee, K. H. Jung, R. K. Vatsa, J. P. Mittal, and H. R. Volpp, Chem. Phys. Lett. **358**, 314 (2002).
[42] K. Seki and H. Okabe, J. Phys. Chem. **97**, 5284 (1993).
[43] W. B. DeMore, S. P. Sander, D. M. Golden, R. F. Hampson, Jr., M. J. Kurylo, C. J. Howard, A. R. Ravishankara, C. E. Kolb, and M. J. Molina, *Chemical Kinetics and Photochemical Data for Use in Stratospheric Modeling* (NASA/JPL, Pasadena, 1997).
[44] A. A. Turnipseed, G. L. Vaghjiani, J. E. Thompson, and A. R. Ravishankara, J. Chem. Phys. **96**, 5887 (1992).
[45] A. Schiffman, D. D. Nelson, Jr., and D. J. Nesbitt, J. Chem. Phys. **98**, 6935 (1993).
[46] L. S. Rothman, C. P. Rinsland, A. Goldman *et al.*, J. Quant. Spectrosc. Radiat. Transf. **60**, 665 (1998).
[47] G. H. Dieke and H. M. Crosswhite, J. Quant. Spectrosc. Radiat. Transf. **2**, 97 (1962).
[48] J. Luque and D. R. Crosley, SRI International Report MP 99, 1999.
[49] G. Herzberg, *Molecular Spectra and Molecular Structure* (Van Nostrand, Princeton, NJ, 1950), Vol. 1.
[50] K. F. Palmer, M. E. Mickelson, and K. N. Rao, J. Mol. Spectrosc. **44**, 131 (1972).
[51] D. R. Guyer, L. Hüwel, and S. R. Leone, J. Chem. Phys. **79**, 1259 (1983).
[52] J. M. Hossenlopp, D. T. Anderson, M. W. Todd, and M. I. Lester, J. Chem. Phys. **109**, 10707 (1998).
[53] J. A. Beswick and J. Jortner, Adv. Chem. Phys. **47**, 363 (1981).
[54] M. J. Bramley, S. Carter, N. C. Handy, and I. M. Mills, J. Mol. Spectrosc. **157**, 301 (1993).
[55] M. I. Lester, B. V. Pond, D. T. Anderson, L. B. Harding, and A. F. Wagner, J. Chem. Phys. **113**, 9889 (2000).
[56] G. E. Ewing, J. Phys. Chem. **91**, 4662 (1987).
[57] R. T. Bonn, M. D. Wheeler, and M. I. Lester, J. Chem. Phys. **112**, 4942 (2000).

[58] D. T. Anderson, R. L. Schwartz, M. W. Todd, and M. I. Lester, J. Chem. Phys. **109**, 3461 (1998).
[59] W. H. Green, Jr. and M. I. Lester, J. Chem. Phys. **96**, 2573 (1992).
[60] M. D. Marshall, B. V. Pond, S. M. Hopman, and M. I. Lester, J. Chem. Phys. **114**, 7001 (2001).
[61] M. Peric and S. D. Peyerimhoff, J. Mol. Spectrosc. **212**, 142 (2002).
[62] J. A. Pople, Mol. Phys. **3**, 16 (1960).
[63] J. T. Hougen, J. Chem. Phys. **36**, 519 (1962).
[64] M.-L. Dubernet, P. A. Tuckey, and J. M. Hutson, Chem. Phys. Lett. **193**, 355 (1992).
[65] D. D. Nelson, Jr., A. Schiffman, and D. J. Nesbitt, J. Chem. Phys. **90**, 5455 (1989).
[66] S. R. Langhoff, C. W. Bauschlicher, Jr., and P. R. Taylor, J. Chem. Phys. **91**, 5953 (1989).
[67] M. D. Wheeler, M. Tsiouris, M. I. Lester, and G. Lendvay, J. Chem. Phys. **112**, 6590 (2000).
[68] M. J. Lakin, D. Troya, G. C. Schatz, and L. B. Harding, J. Chem. Phys. **119**, 5848 (2003).
[69] D. M. Medvedev, S. K. Gray, E. M. Goldfield, M. J. Lakin, D. Troya, and G. C. Schatz, J. Chem. Phys. **120**, 1231 (2004).